First two pages: a few extra comments on the Curve of Growth (Jelle's lecture)

Photospheric X-ray absorption spectrum from surface of neutron star (?)

XMM/RGS: Cumulative spectrum of 30 X-ray bursts

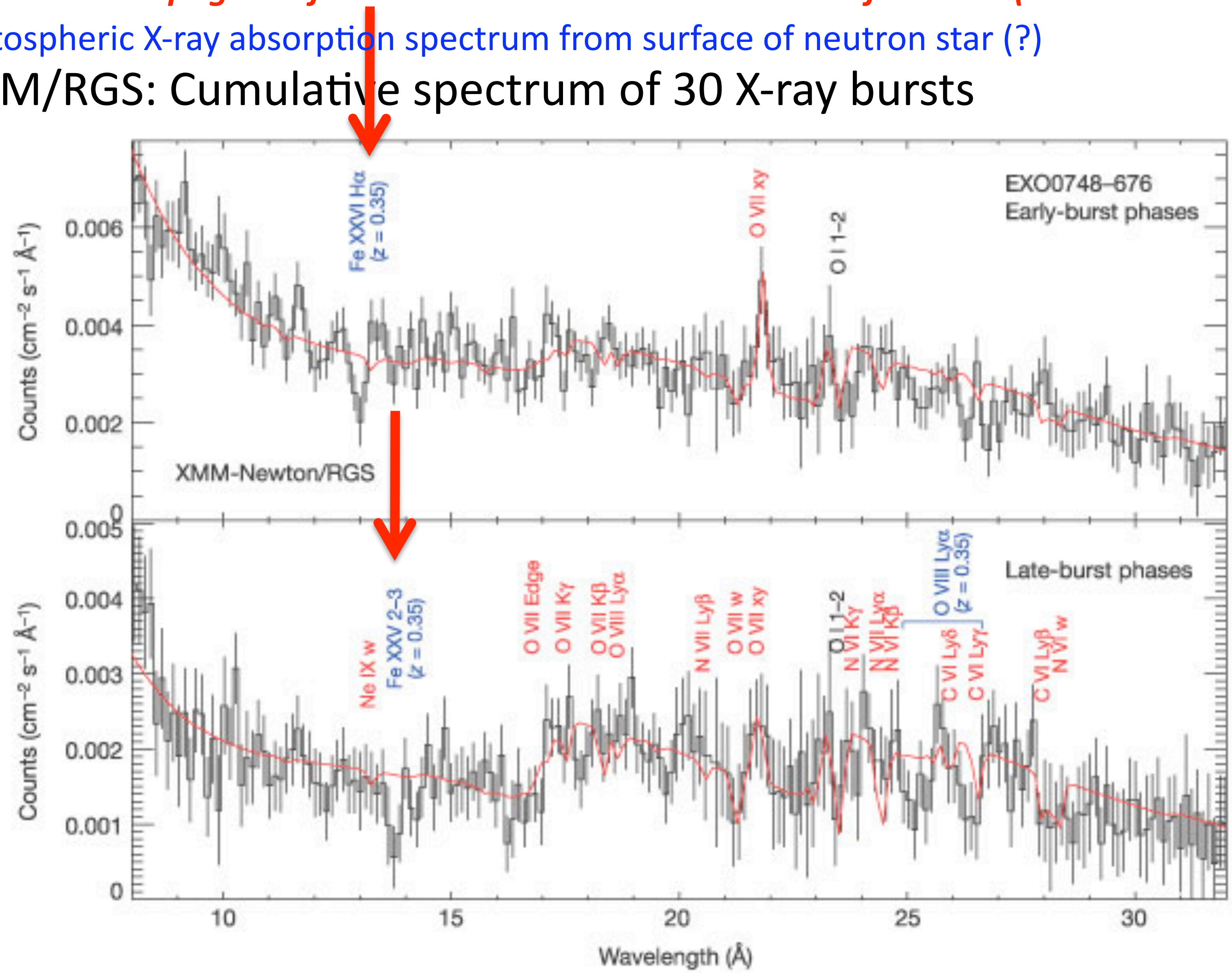

If correct identification: gravitational redshift!

$z = 0.35$

(Cottam, Paerels, & Mendez, 2002, *Nature*, **420**, 51)

Curve of growth for Fe XXVI n=2-3 (absorbing layer approximation)

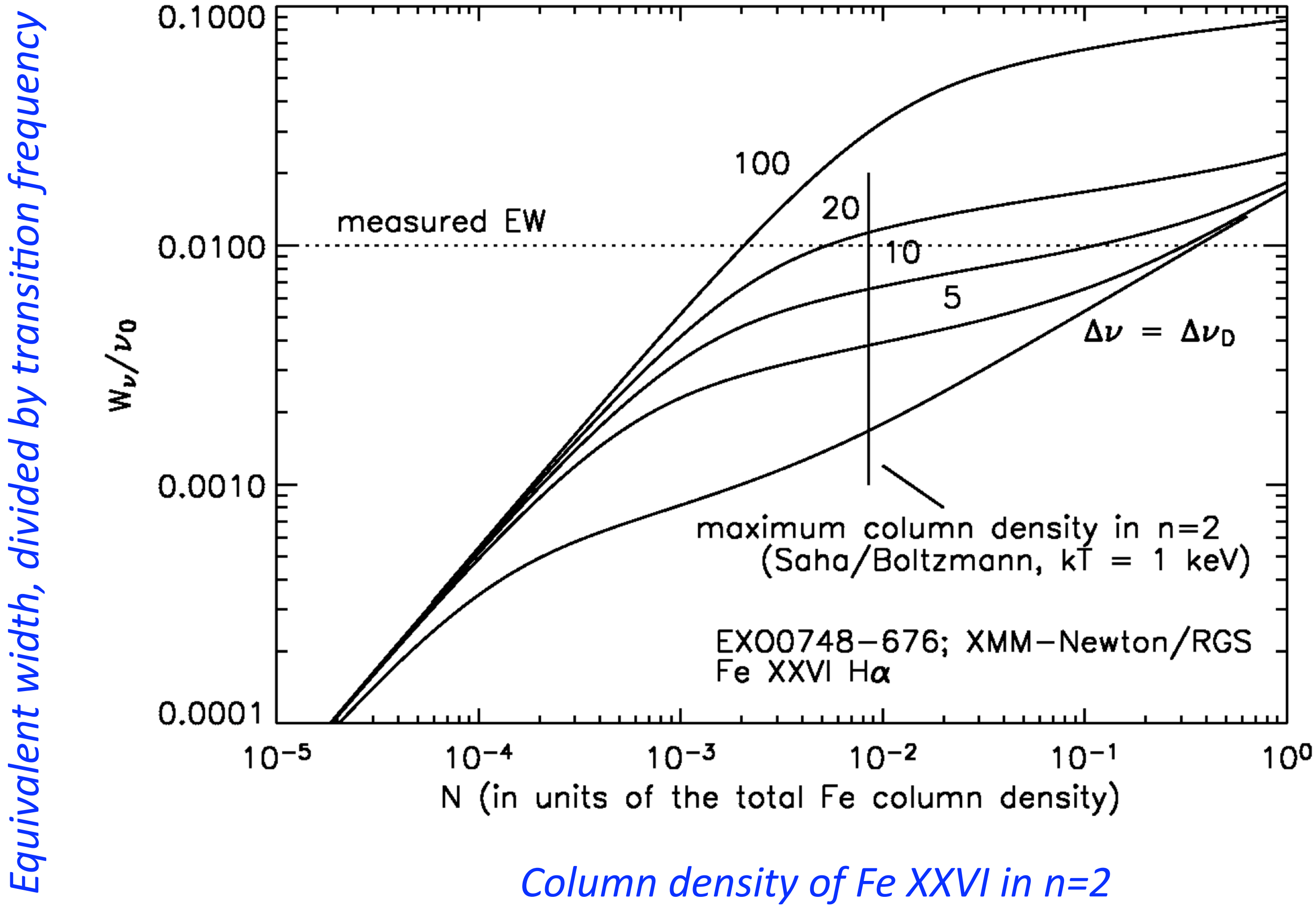

Also: slow spin (fortuitous)!

ν = 45 Hz, Villareal & Strohmayer, 2004, *ApJ*, **614**, L121

First Astro-H Science Summer School

Minakami Onsen, August 19-21, 2010

5. High Resolution Spectroscopy

Frits Paerels[(1)], Jelle Kaastra[(2)], and Randall Smith[(3)]

(1) Columbia University
(2) SRON Utrecht
(3) Harvard-Smithsonian CfA

Part 1:

- High Resolution Spectroscopy
- Historical Precedent: grating spectroscopy with Chandra and XMM
- Types of Equilibrium: simple diagnostics
- Basics of He-triplet Spectroscopy
- T-diagnostics: collisional and radiation-dominated plasmas

Brief Break

Part 2:

- n-diagnostics
- Non-equilibrium situations
- Radiative transfer issues

NB: I will be discussing emission spectroscopy; Jelle will address absorption

What is 'high' in 'high resolution' ?

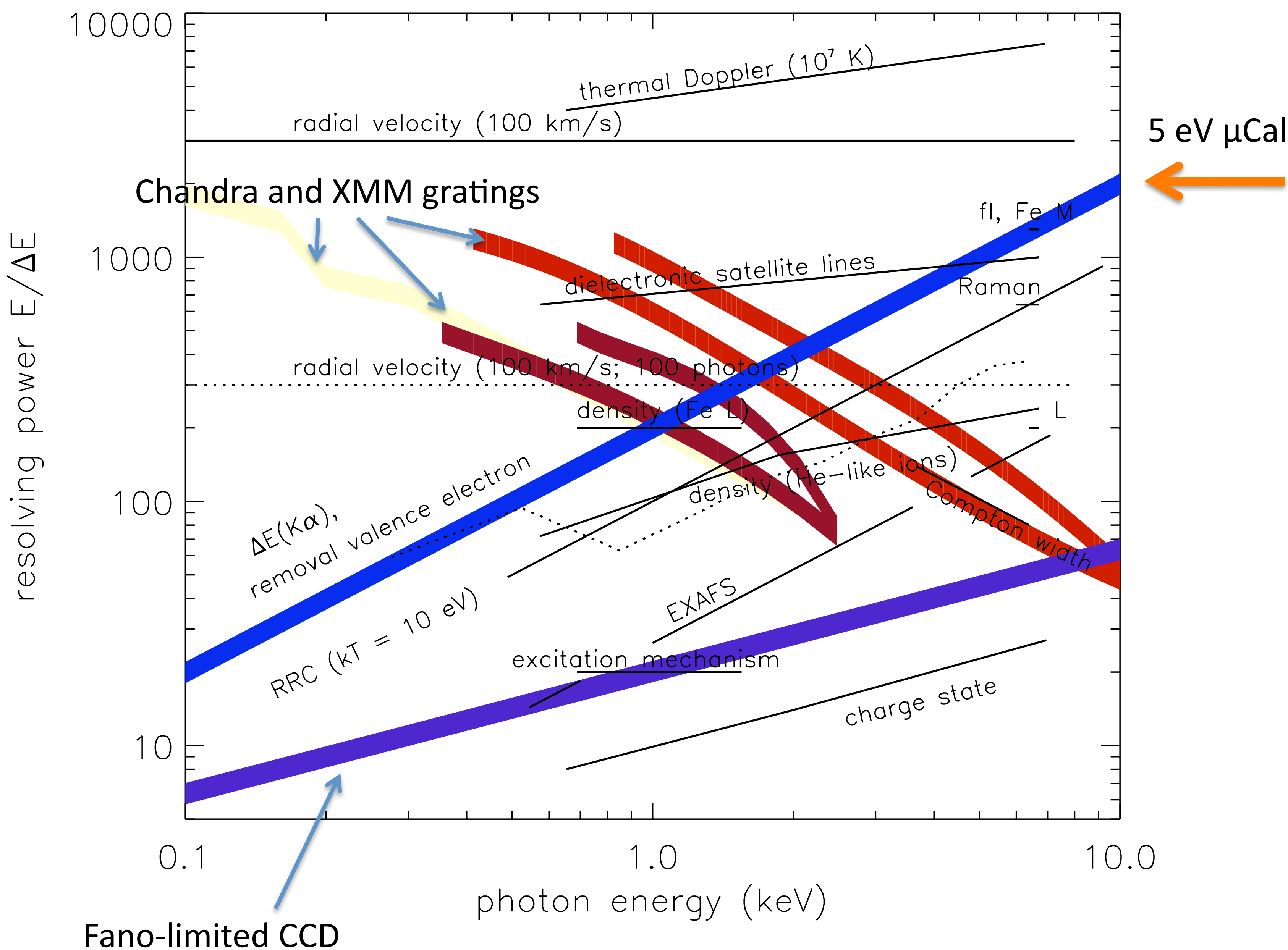

Historical Context

A few crystal spectrometer experiments; most notably *Einstein* FPCS (Canizares, MIT); First ‘resolved’ spectroscopy in X-ray astronomy (resolve elements, charge states)

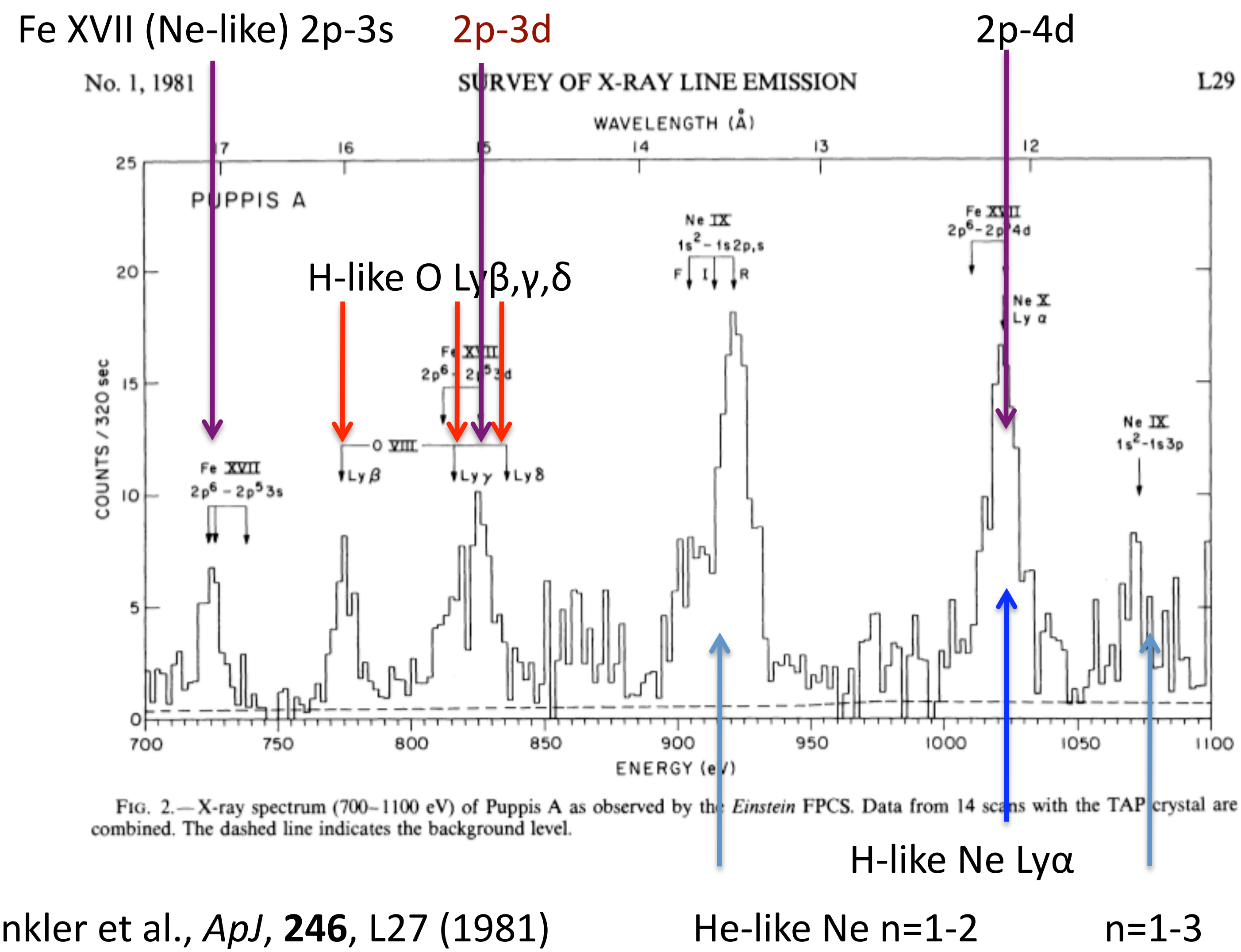

FIG. 2.—X-ray spectrum (700–1100 eV) of Puppis A as observed by the *Einstein* FPCS. Data from 14 scans with the TAP crystal are combined. The dashed line indicates the background level.

Winkler et al., *ApJ*, **246**, L27 (1981)

But FPCS was inefficient.
Einstein and EXOSAT had transmission grating spectrometers;
likewise: novel, but inefficient

ASCA was the first 'general purpose' spectrometer; CCDs resolve element, ionization stage, and some further spectral detail

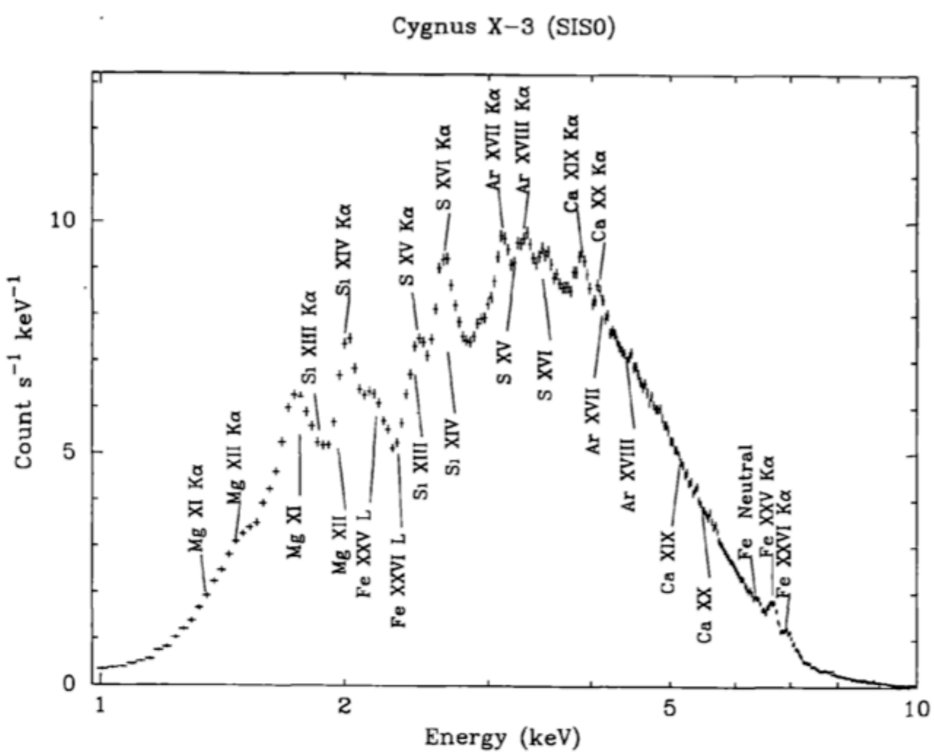

Fig. 1. Phase-averaged energy spectrum of Cyg X-3 obtained by SIS 0. The emission lines from He-like and H-like ions and electron binding energies for K-shell and L-shell of H-like and He-like ions are indicated.

Kawashima and Kitamoto, *PASJ*, **48**, L113 (1996)

Truly general purpose, fully resolved astrophysical spectroscopy (but point sources only!):
Grating spectrometers in Chandra, XMM:

NB: 5 eV microcalorimeter spectrum will appear almost the same!

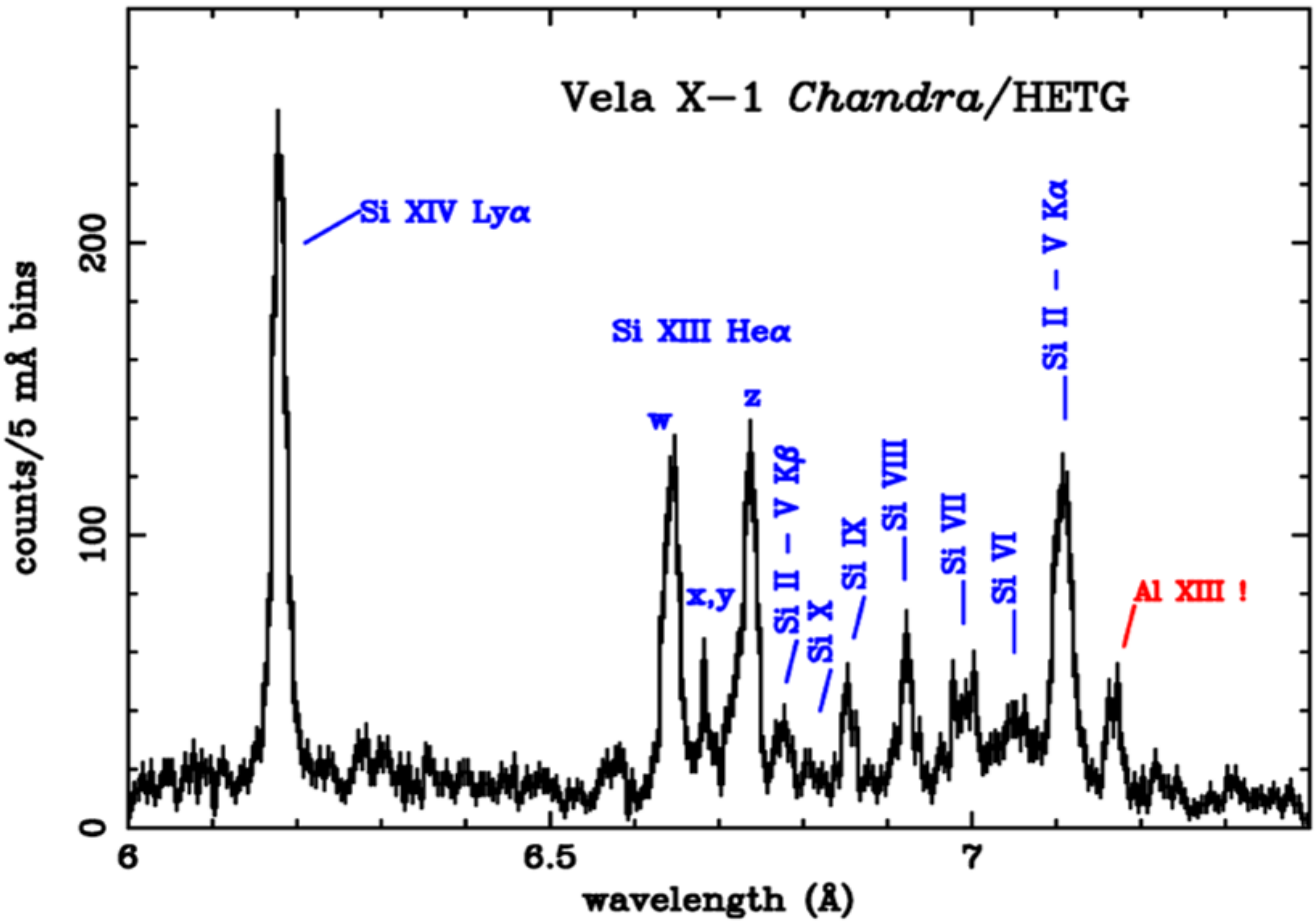

Watanabe et al., *ApJ*, **651**, 421 (2006)

Types of Equilibrium

Very roughly: *collisional*, and *radiation-driven* plasmas

‘hot gas’
(unspecified energy source)

Cool, recombining plasmas

Very simple, robust spectroscopic signature of recombining plasma:

Radiative Recombination Continua (RRC)

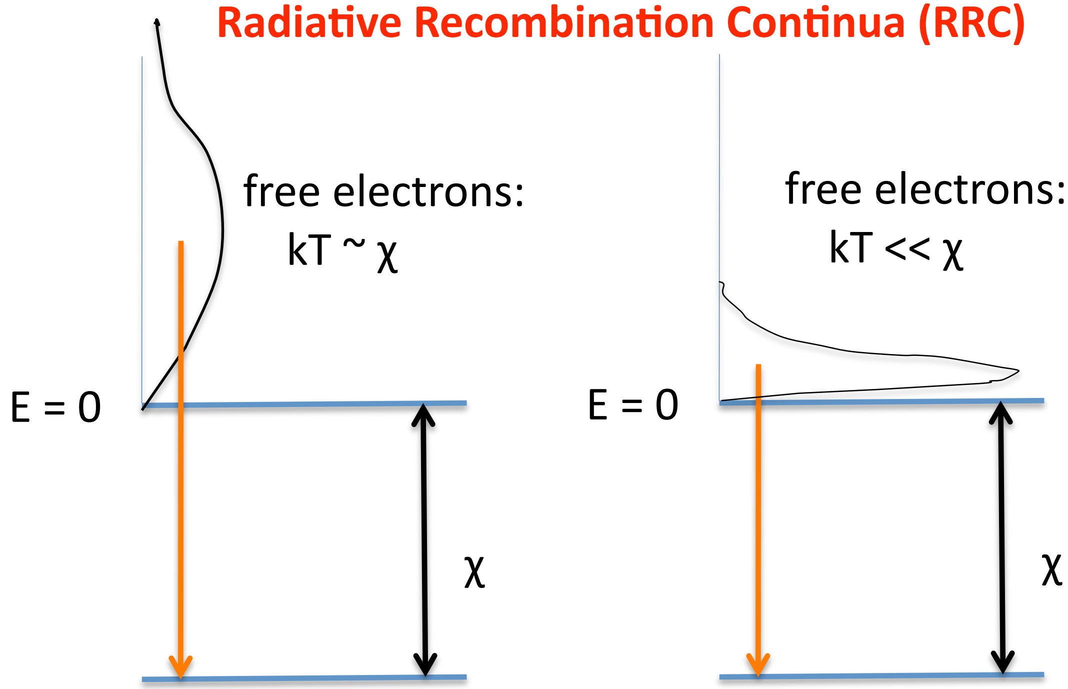

Collisional equilibrium

Photoionization equilibrium

RRC's in Cygnus X-3

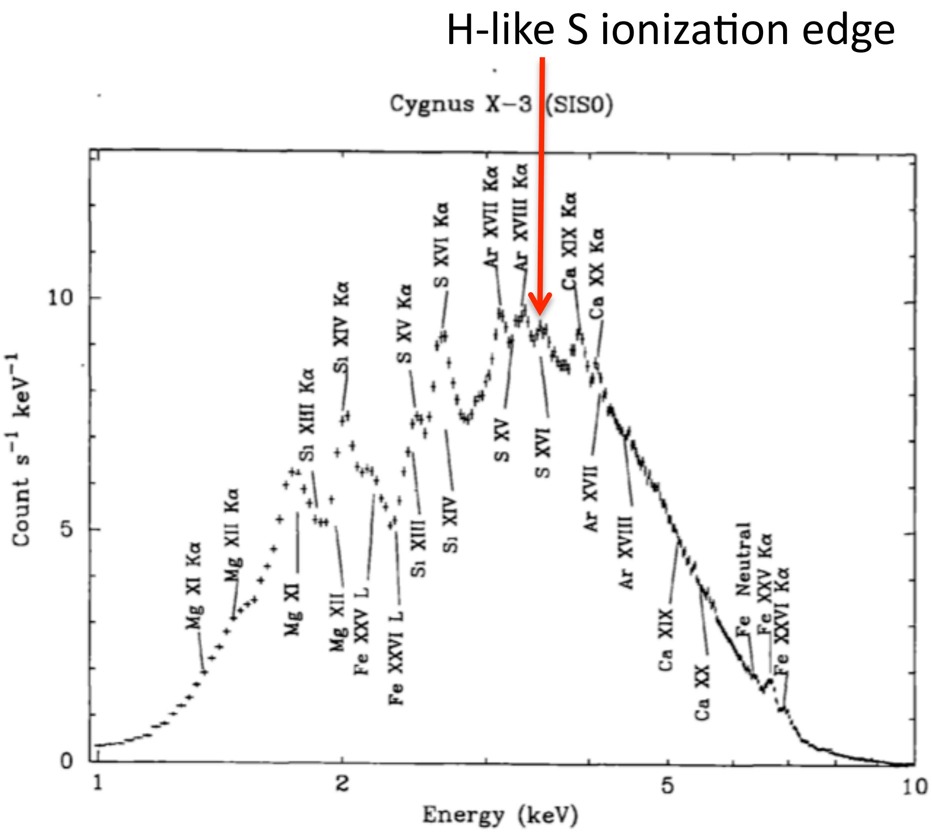

Fig. 1. Phase-averaged energy spectrum of Cyg X-3 obtained by SIS 0. The emission lines from He-like and H-like ions and electron binding energies for K-shell and L-shell of H-like and He-like ions are indicated.

Cygnus X-3 with Chandra HETGS

Fully resolved RRC's;
Width ΔE ~ kT_e ~ few eV

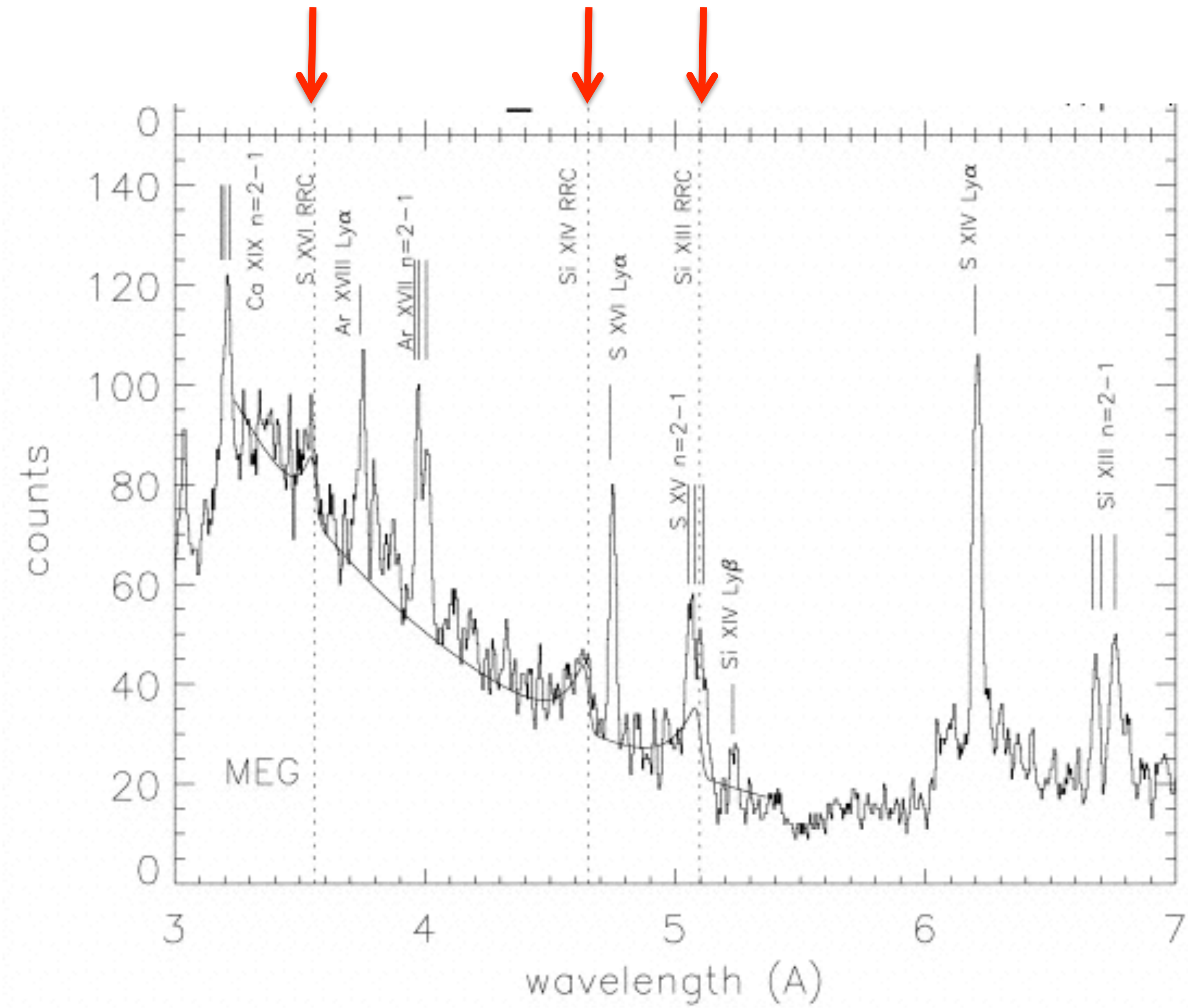

Paerels et al., *ApJL*, **533**, L135 (2000)

Another simple diagnostic to discriminate between collisional excitation and recombination or charge exchange: **the 'series decrement'**

Collisional excitation makes n=1-2 (for example), but can only make much less n=1-3, 4, 5… so flux ratio's (3-1)/(2-1), (4-1)/(2-1), … (the 'decrement') small

Both recombination and charge exchange populate higher-n levels more effectively, leading to relatively stronger higher-order series members ('flat decrement').

Fig. 18. Classical trajectory Monte Carlo model spectra from charge exchange of O^{8+} and H at energies from 1 eV/amu to 100 keV/amu (adapted from Otranto et al. ref. 130). High-*n* emission is strongly enhanced at low energies but nearly vanishes as the collision energy approaches E_{crit}.

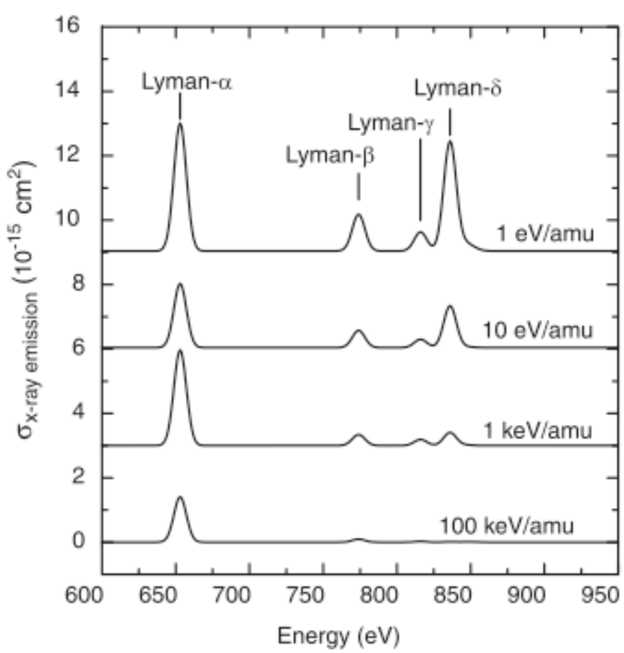

Wargelin, Beiersdorfer, Brown, *Can.J.Phys.*, **86**, 151 (2008)

Basics of He-like 'Triplet' Spectroscopy

write total wavefunction as product ψ(spatial).ψ(spin) = $\psi(\ell_1,\ell_2).\psi(s_1,s_2)$

Two electrons: can have |↑↑>, |↓↓>, |↑↓>, |↓↑>. But these are not all eigenstates of ***J***. Eigenstates of ***J*** are:

|↑↑>, |↓↓>, |↑↓> + |↓↑> (symmetric in the spins, total spin 1) **'triplet'**

|↑↓> − |↓↑> (antisymmetric in the spins, total spin 0) | **'singlet'**

He-like ion

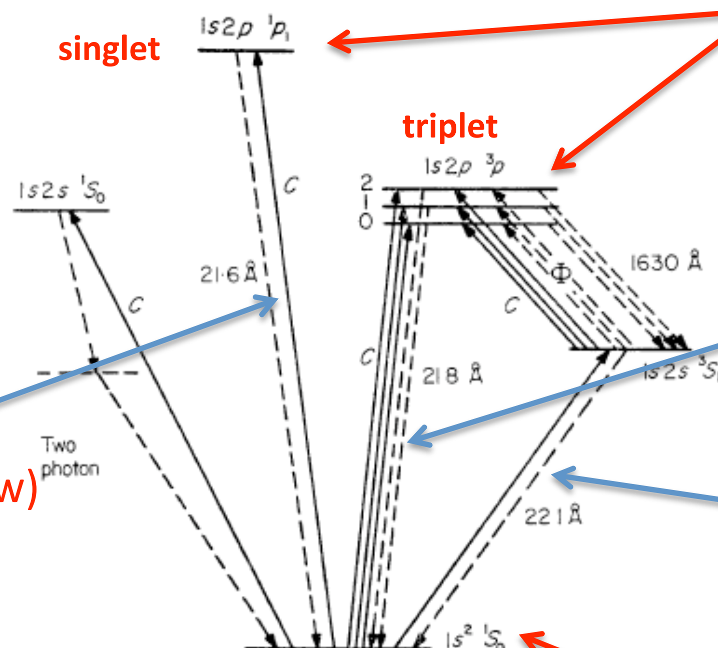

FIG. 1. *The He-like ion, showing those terms and processes involved in the present analysis. The wavelengths indicated apply to the case of oxygen* VII.

1s 2p; ***L*** = ***l***$_1$ + ***l***$_2$ = 1, so: *P* ;
four electron spin possibilities

'intercombination line(s)' (xy)
(between triplet and singlet States; involves spin flip)

'resonance line' (w)

'forbidden line' (z)
(LS forbidden)

Ground: space-*symmetric*, must be spin-*antisymmetric*, so s = 0 (2s+1 = 1; **singlet**)

Gabriel and Jordan, 1969, *MNRAS*, **145**, 241

H-LIKE SPECIES

Ion	Lyα₁		Lyα₂		K-edge	
	λ (Å)	E (keV)	λ (Å)	E (keV)	λ (Å)	E (keV)
C VI	33.7342	0.36754	33.7396	0.36747	25.3033	0.489993
N VII	24.7792	0.50036	24.7846	0.50024	18.5871	0.667046
O VIII	18.9671	0.65368	18.9725	0.65348	14.2280	0.871410
Ne X	12.1321	1.02195	12.1375	1.02150	9.10177	1.36220
Na XI	10.0232	1.23697	10.0286	1.23631	7.52011	1.64870
Mg XII	8.41920	1.47264	8.42461	1.47169	6.31714	1.96266
Al XIII	7.17091	1.72899	7.17632	1.72769	5.38093	2.30414
Si XIV	6.18043	2.00608	6.18584	2.00432	4.63808	2.67318
S XVI	4.72735	2.62270	4.73276	2.61970	3.54830	3.49419
Ar XVIII	3.73110	3.32299	3.73652	3.31817	2.80113	4.42622
Ca XX	3.01848	4.10750	3.02390	4.10014	2.26668	5.46986
Fe XXVI	1.77802	6.97316	1.78344	6.95197	1.33637	9.27769

Lines: Johnson, W. R., & Soff, G. 1985, Atom. Data Nucl. Data Tables, **33**, 405

HE-LIKE SPECIES

Ion	w(resonance)		x(intercombo)		y(intercombo)		z(forbidden)		K-edge	
	λ (Å)	E (keV)	λ (Å)	E (keV)	λ (Å)	E (keV)	λ (Å)	E (keV)	λ (Å)	E (keV)
C V	40.2674	0.307902	40.7280	0.304420	40.7302	0.304404	41.4718	0.298960	31.63	0.392
N VI	28.7800	0.430800	29.0819	0.426328	29.0843	0.426293	29.5346	0.419793	22.46	0.552
O VII	21.6015	0.573961	21.8010	0.568709	21.8036	0.568641	22.0974	0.561080	16.78	0.739
Ne IX	13.4473	0.922001	13.5503	0.914992	13.5531	0.914803	13.6984	0.905100	10.37	1.196
Na X	11.0029	1.12683	11.0802	1.11897	11.0832	1.11867	11.1918	1.10781	8.463	1.465
Mg XI	9.16875	1.35225	9.22817	1.34354	9.23121	1.34310	9.31362	1.33121	7.037	1.762
Al XII	7.75730	1.59829	7.80384	1.58876	7.80696	1.58812	7.87212	1.57498	5.944	2.086
Si XIII	6.64795	1.86500	6.68499	1.85467	6.68819	1.85378	6.73949	1.83967	5.085	2.438
S XV	5.03873	2.46062	5.06314	2.44876	5.06649	2.44714	5.10067	2.43074	3.846	3.224
Ar XVII	3.94907	3.13958	3.96587	3.12628	3.96936	3.12353	3.99415	3.10414	3.009	4.121
Ca XIX	3.17715	3.90237	3.18910	3.88775	3.19275	3.88330	3.21103	3.86120	2.417	5.129
Fe XXV	1.85040	6.70040	1.85541	6.68231	1.85952	6.66754	1.86819	6.63659	1.404	8.828

Lines: Drake, G. W. 1988, Can. J. Phys., **66**, 586
Edges: HULLAC, except for Na & Al (Verner et al. 1996, ApJ, **465**, 487)

Courtesy Masao Sako (UPenn)

Appearance of the triplets: example: OVII in Capella with Chandra HETGS

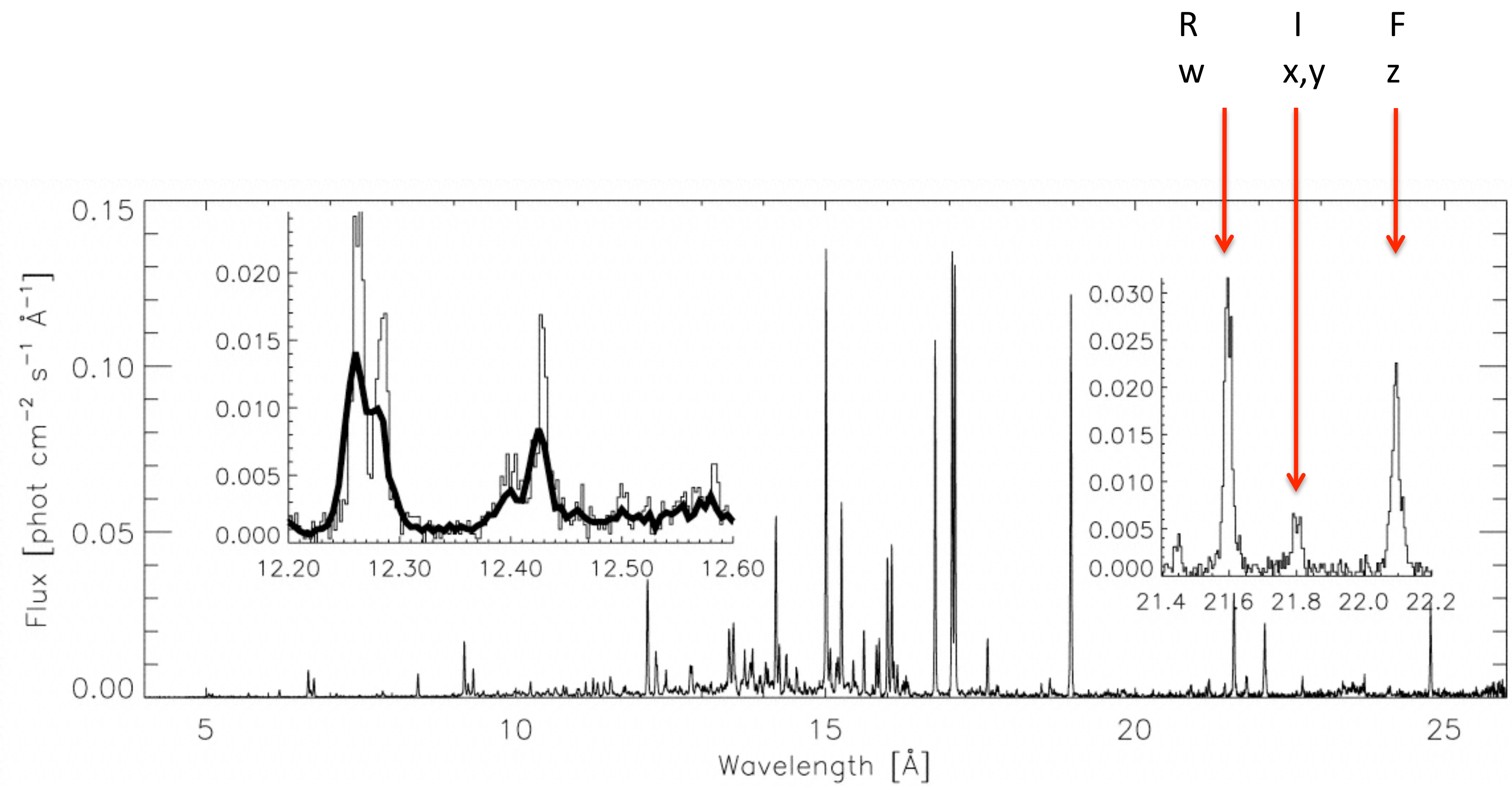

Canizares *et al*., 2000, *ApJL*, **539**, L41

First thing to note: resonance line is bright in collisional equilibrium plasmas

Spectroscopic power of He-like triplet spectroscopy due to the fact that upper levels for w, x,y, and z populated mostly by different mechanicsms, with different temperature dependence

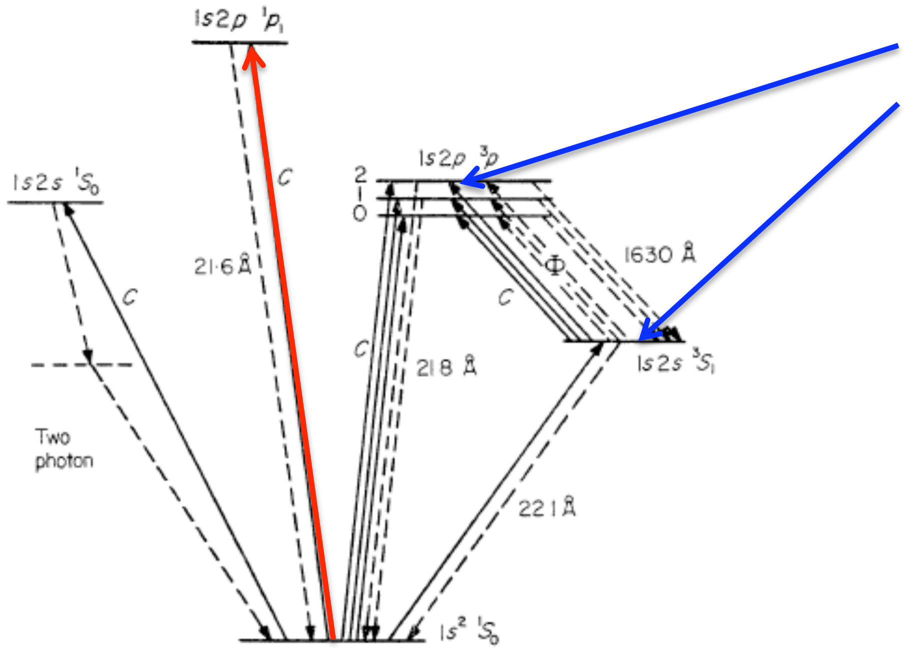

FIG. 1. *The He-like ion, showing those terms and processes involved in the present analysis. The wavelengths indicated apply to the case of oxygen* VII.

Example: coronal (collisional) equilibrium:
CX to 1s2p $^1S_0$ dominates over recombination to 1s2p ^3P, 1s2s $^3S_1$
NB: *z* not collisionally excited for ~ same reason it's radiatively forbidden!

We will see many more applications of He-like triplets as we go along

Electron Temperature Diagnostics

Collisional plasmas: Fe L ionization balance
He-like (I+F)/R ratio
dielectronic satellites
direct ion thermal velocity spectroscopy

Fe L ionization balance: simple- ionization states range from 2×10^6-3×10^7 K
Fe L lines are bright !

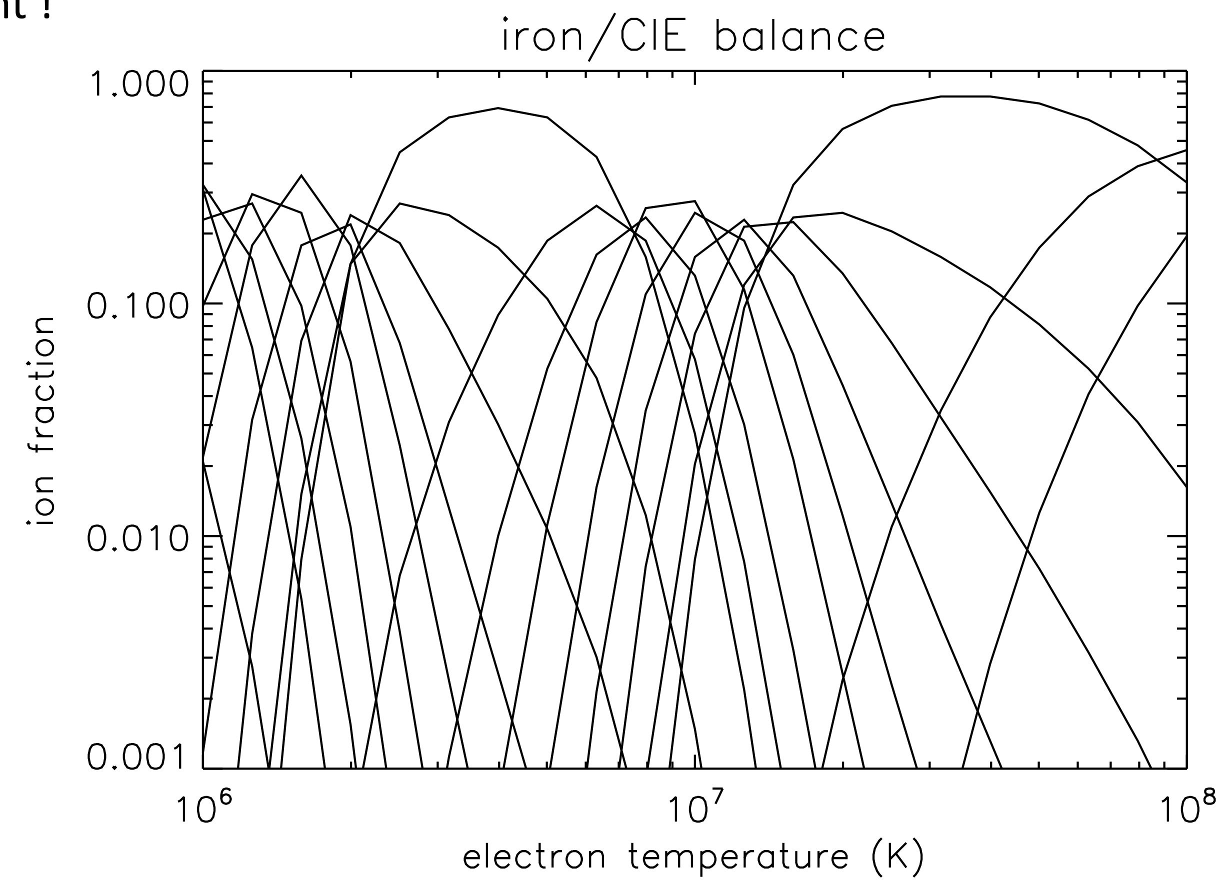

Based on Arnaud and Raymond, *ApJ*, **398**, 394 (1992)

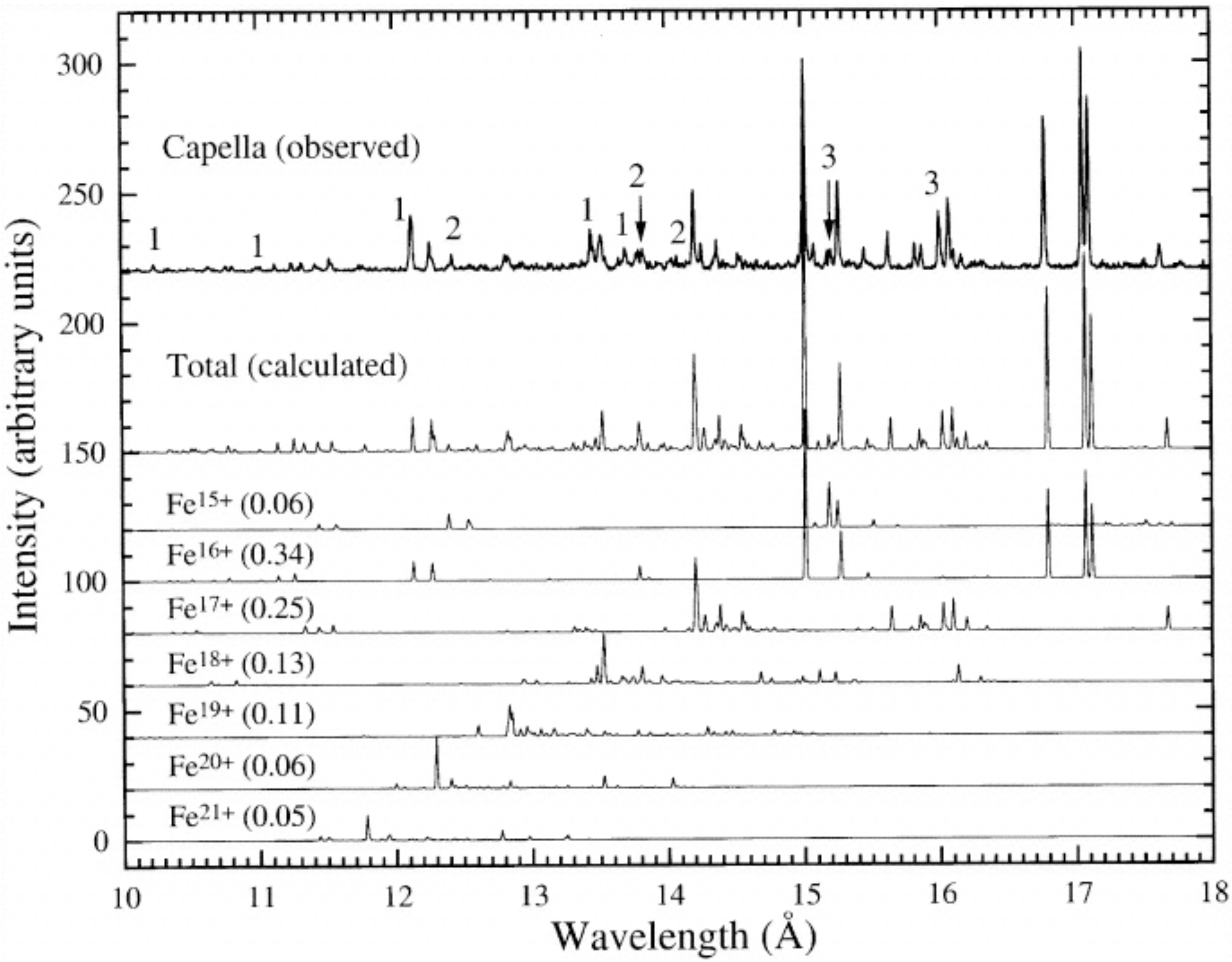

Appearance of the Fe L collisional spectrum; Capella/XMM-Newton RGS
Behar, Cottam, and Kahn, *ApJ*, **548**, 966 (2001)

(something similar is true for photoionization equilibrium-
but balance is usually 'messier'-more ionization stages simultaneously present)

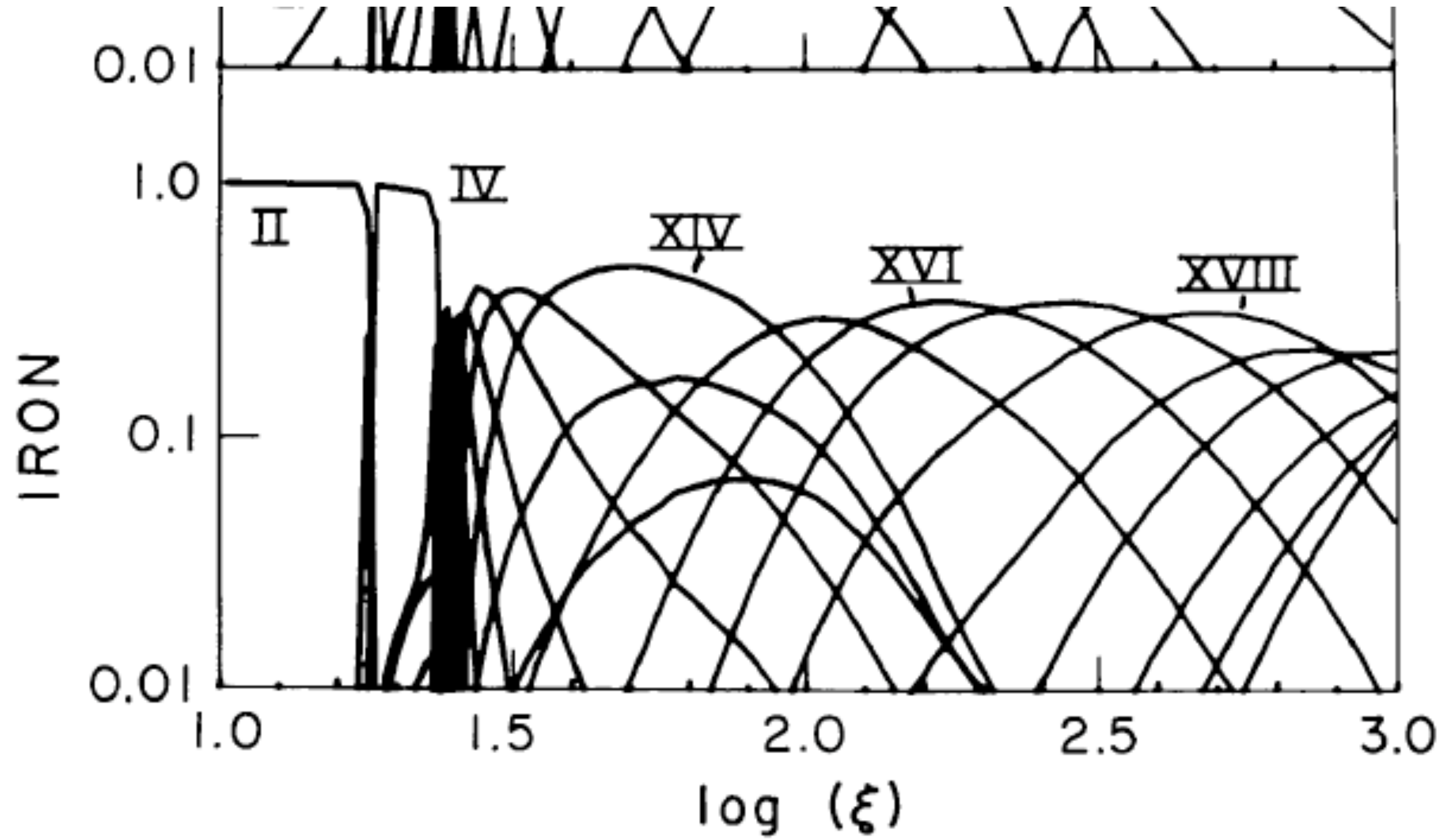

Photoionization equilibrium balance for E^{-1} powerlaw photon spectrum;
Kallman and McCray, *ApJS*, **50**, 263 (1982)

Electron temperature from He-like triplet spectroscopy

Upper levels of the resonance, and forbidden+intercombinaton lines mostly populated by collisional excitation, and recombination, respectively. CX and RR+DR have different T_e-dependence:

ratio **G = (x+y+z)/w** is T_e-sensitive:
High T_e favors CX

Careful: blending with other transitions may bias simple measurement of G. Need to model emission spectrum, in practice.

Different curves are for different ratio's of H-to He-like ion densities; allows for deviations from pure CIE. Lowest curve is pure CIE; higher curves apply to photoionization cases.

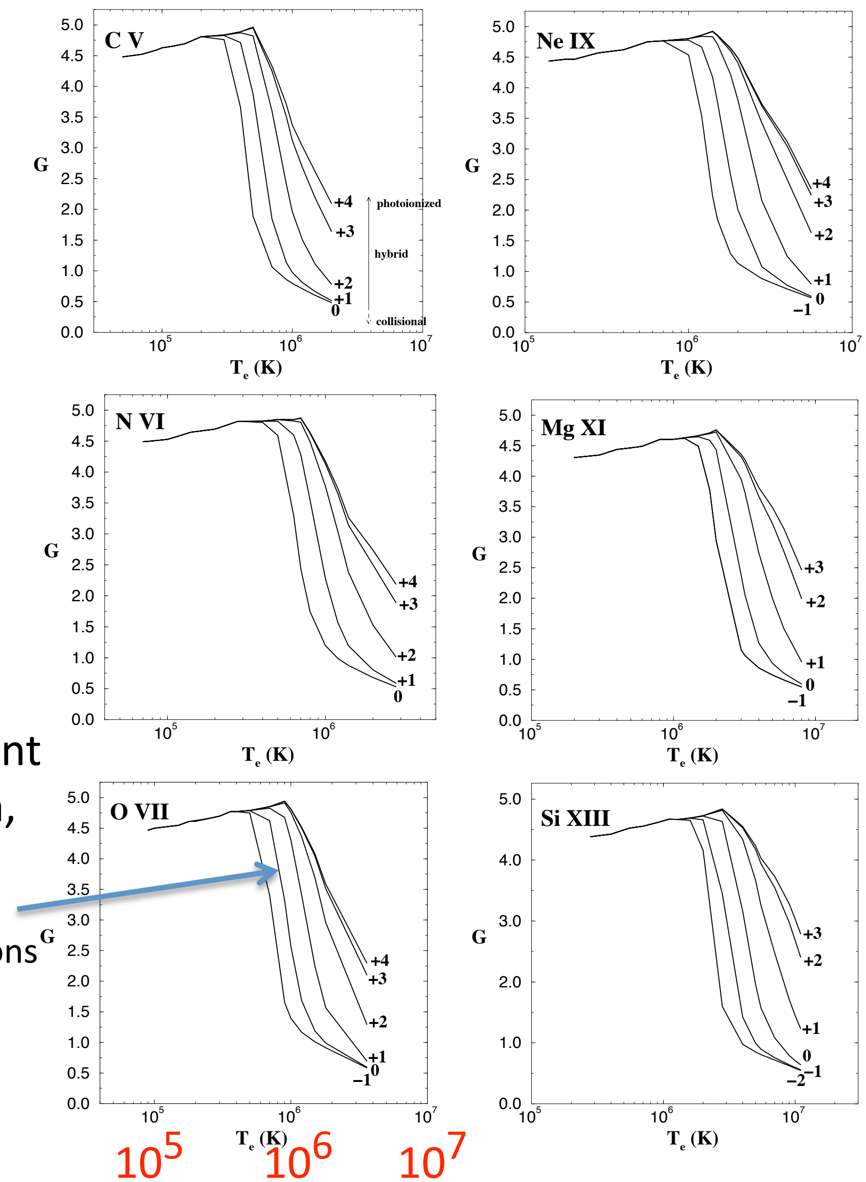

Fig. 7. G (=(x+y+z)/w) is reported as a function of electronic temperature (T_e) for C V, N VI, O VII, Ne IX, Mg XI, and Si XIII in the density range where **G** is not dependent on density (see §3.2). The number (m) associated to each curves means $X_{ion}=10^m$, where X_{ion} is the ratio of H-like ions over He-like ions. As an example for Oxygen (Z=8) it corresponds to ratio of the relative ionic abundance of O VIII/O VII ground state population.

Porquet & Dubau, *A&AS*, **143**, 495 (2000)

Electron temperature from Dielectronic Satellite Transitions

Presence of 'spectator electron' shifts levels a little bit (Coulomb shielding of nuclear field): the emission line will be slightly to lower energy as compared to equivalent line in ion +z: dielectronic 'satellite' to line in ion +z

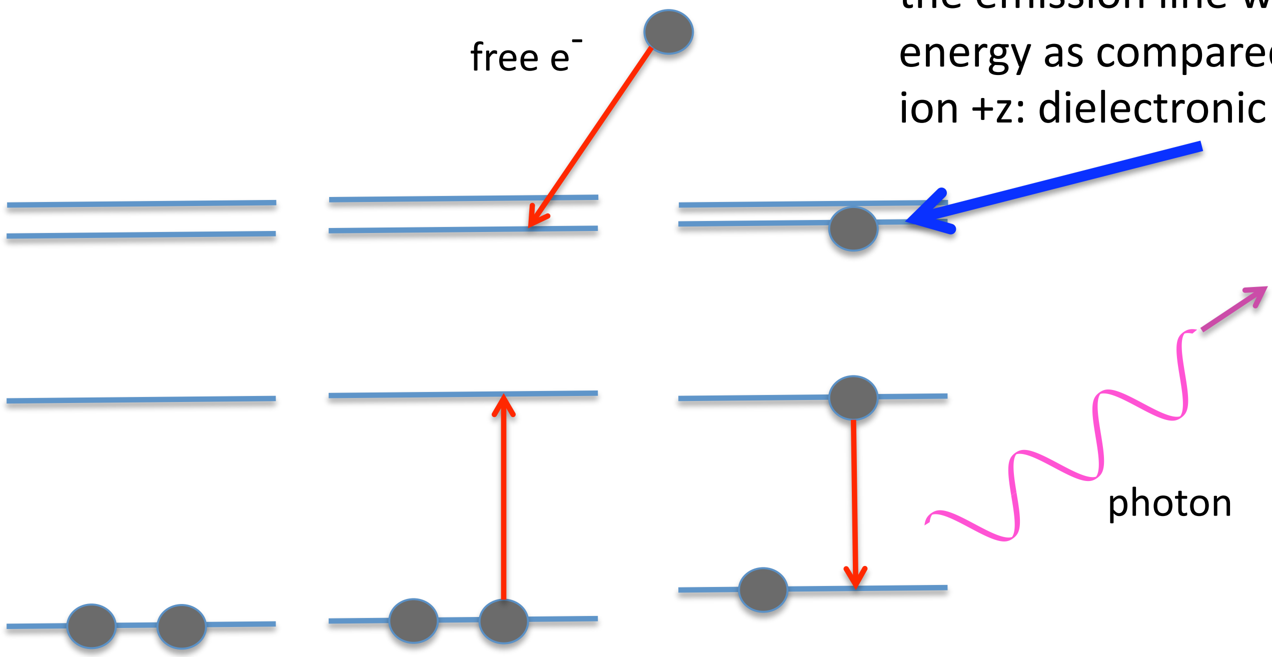

Ion stage +z
(*e.g.* He-like)

Ion stage +(z-1)
(*e.g.* Li-like)

dielectronic recombination

Resonance line *w* will be collisionally excited, the dielectronic satelite excited by DR; both processes different T_e sensitivity: **T_e diagnostic**

Also: both line emissivities scale with n_e $n_{He\text{-}like}$: no dependence on ion balance!

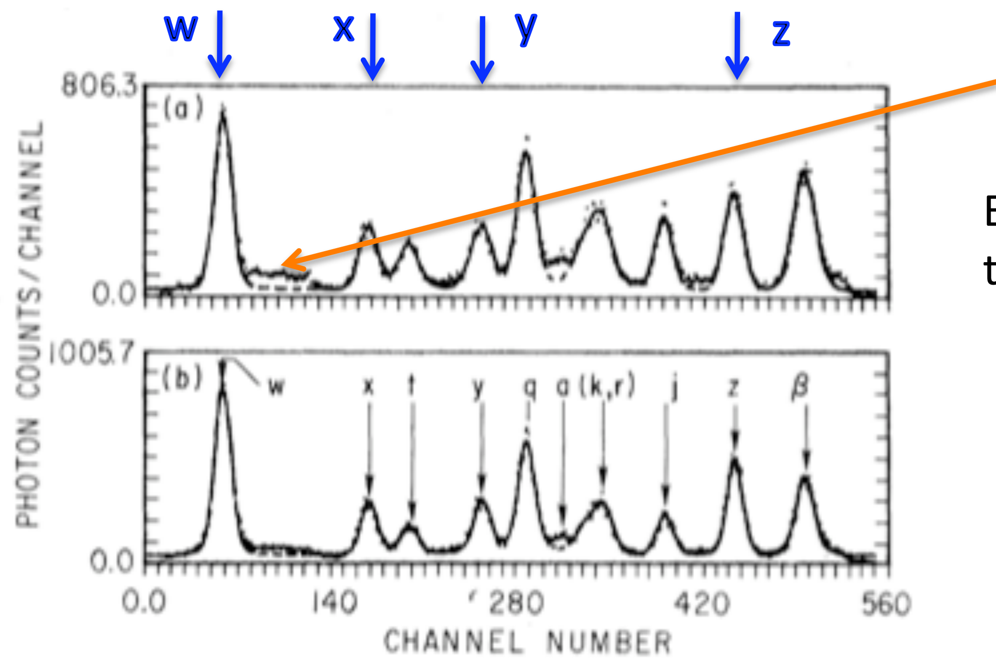

DR satellites to *w*

Example: He/Li-like Fe,
thermal plasma at 1.65 and 2.30 keV

FIG. 1. (a), (b) Dielectronic satellite spectrum of Fe XXV as recorded by a multichannel analyzer from PLT for a central electron temperature of 1.65 and 2.30 keV, respectively. The photon energy decreases with increasing channel number. The conversion gain is 0.18 eV/channel. *w* indicates the Fe XXV $K\alpha$ resonance line at 1.8500 Å. Also shown (solid curve) is the result of a least-squares fit of Voigt functions to the raw data of the most prominent peaks.

Bitter et al., *PRL*, **43**, 129 (1979)

Photoionized and Recombining Plasmas: electron temperature from shape of the RRC

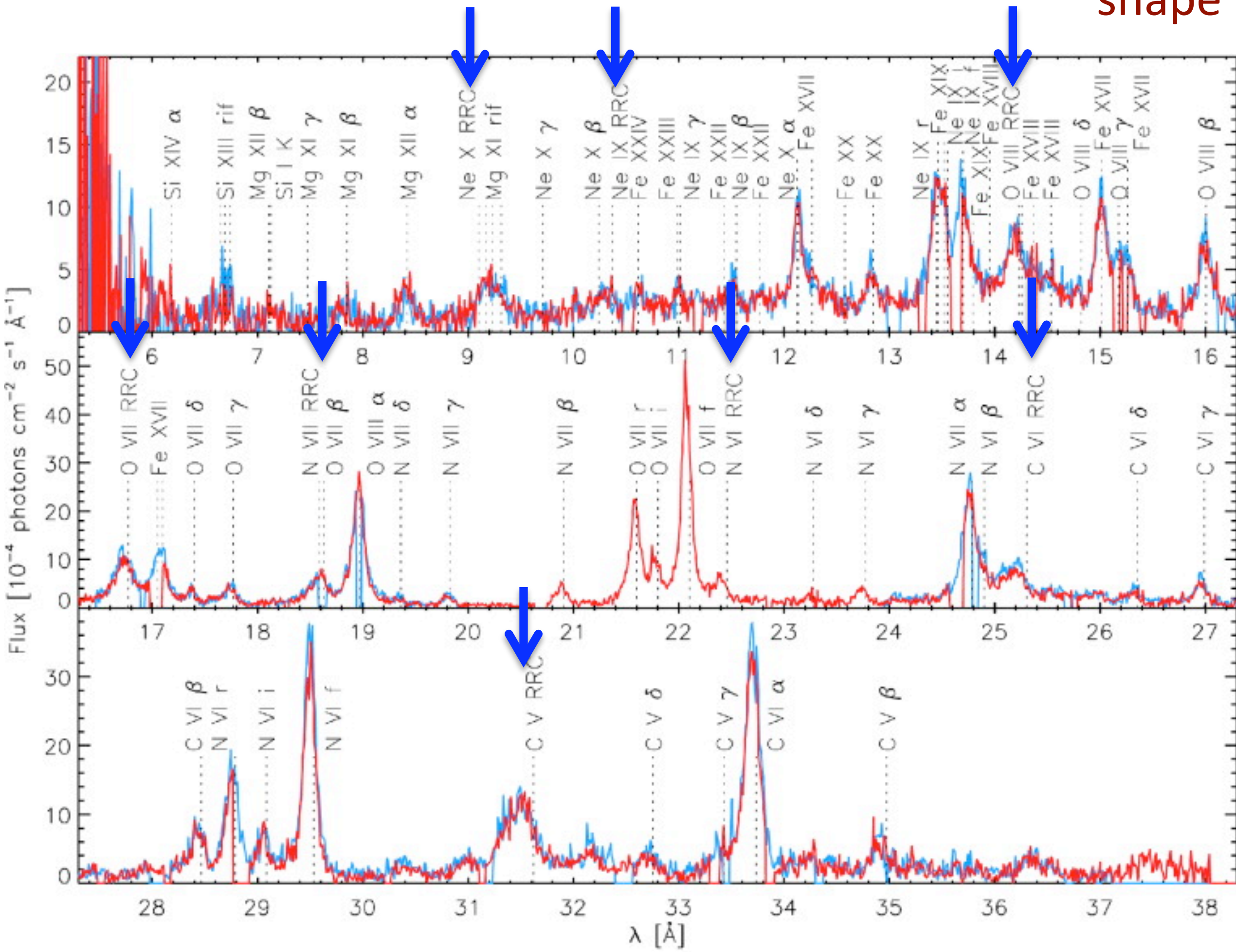

NGC 1068 with XMM-Newton RGS; Kinkhabwala et al., *ApJ*, **575**, 732 (2002)

Shape of RRC directly maps out shape of the free electron Maxwell distribution!

Direct Ion thermal Doppler Broadening Spectroscopy

m: ion mass
Z: nuclear charge
$\mathcal{R}$: Rydberg energy

Thermal Doppler width of Lyα (rms):

$$\sigma = \left(\frac{kT}{mc^2}\right)^{1/2} E_0 \approx \left(\frac{kT}{2m_p Z c^2}\right)^{1/2} \times \frac{3}{4}\mathcal{R}Z^2$$
$$= 2.9\, T_8^{1/2}(Z/26)^{3/2}\ \mathrm{eV}$$

$3^2 + 7^2 = 7.6^2$ so this is **feasible with Astro-H in the Fe K band** at kT_e ~ 10 keV;
but not at lower *Z* (e.g. Si K width is sub-eV at T_8 ~ 0.1)

Need to know the shape of the response to reasonable accuracy
(this example suggests ~< 5% of the width of the response)

Electron Density Diagnostics

F/I ratio in He-like triplets

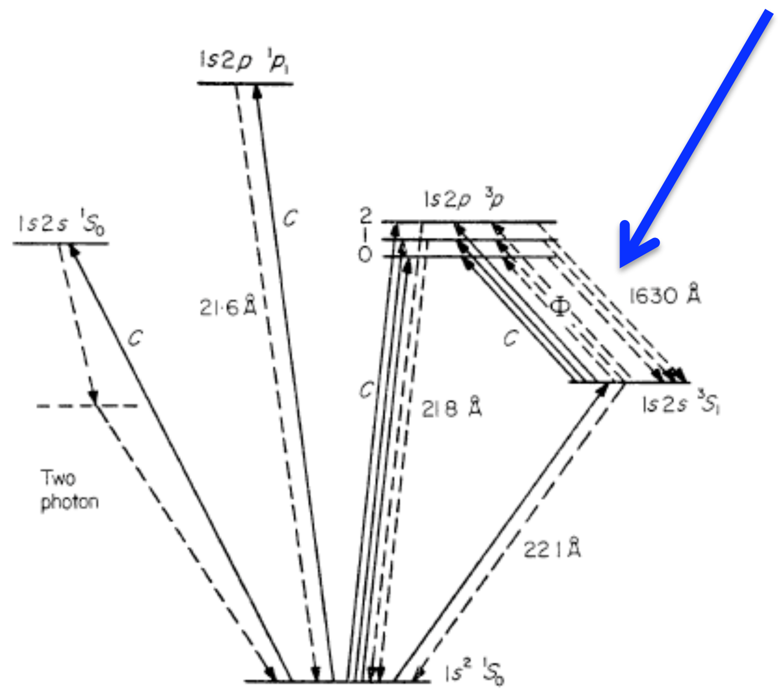

FIG. 1. *The He-like ion, showing those terms and processes involved in the present analysis. The wavelengths indicated apply to the case of oxygen* VII.

At **high density**, or in presence of **intense UV** field (1630 Å for He-like O; shorter for higher-*Z* elements):
population of upper level of z shifts to upper level of x,y:

ratio z/(x+y) is density diagnostic

ratio R = z/(x+y)

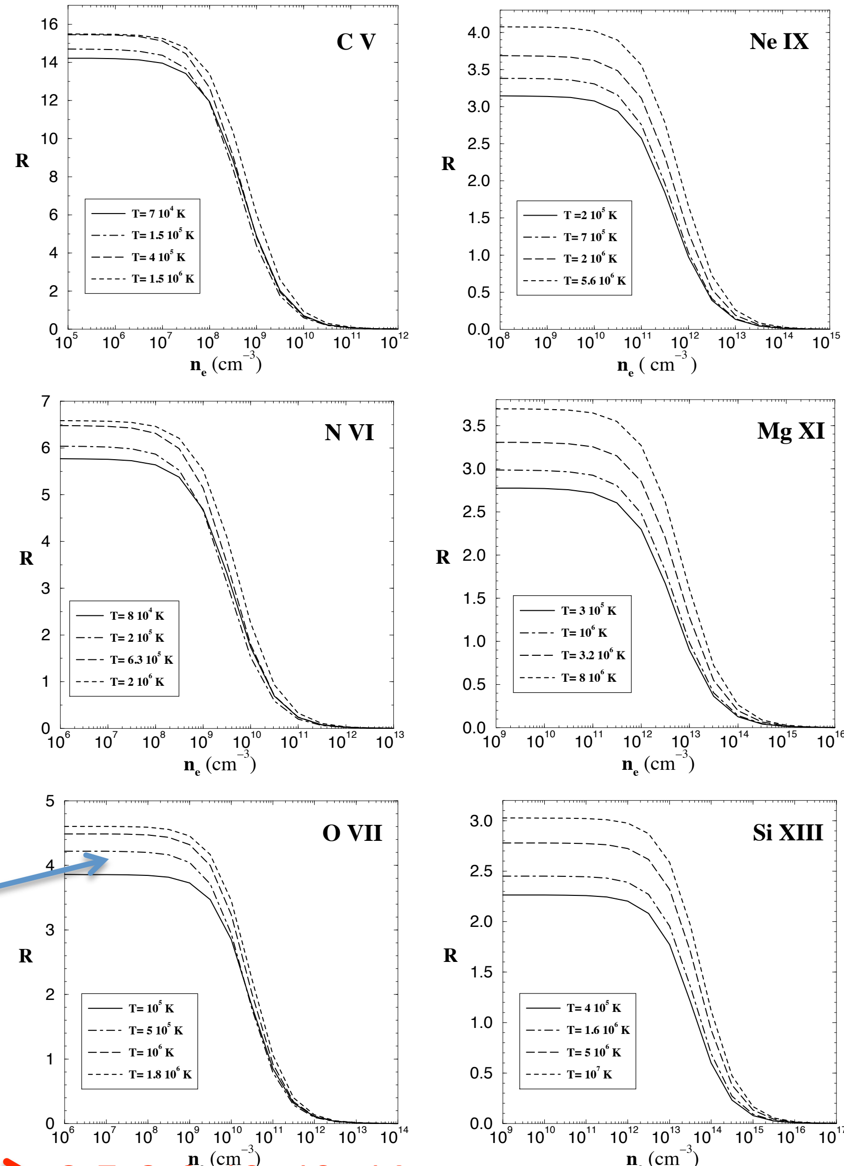

R is weakly T_e-dependent

log n_e (cm^{-3}) → 6 7 8 9 10 12 14

Fig. 8. In case of pure photoionized plasmas (i.e. RR dominant at low temperature and DR dominant at high temperature), **ratio R** (**=z/(x+y)**) is reported as a function of n_e for C V, N VI, O VII, Ne IX, Mg XI, and Si XIII at different electronic temperatures (T_e in Kelvin). For low temperatures (the two first reported here: solid curves and dot-dashed curves), the value of **R** is independent of the value of $\mathbf{X}_{ion}$. As the temperature increases, $\mathbf{X}_{ion}$ is high enough to maintain recombination dominant compared to collisional excitation from the ground level: ~ 10^2 and 10^{3-4} (for increasing temperature: respectively for long-dashed curves and short-dashed curves).

Porquet & Dubau, *A&AS*, **143**, 495 (2000)

Non-equilibrium Situations

We discussed non-equilibrium plasmas yesterday; what are the spectroscopic diagnostics of deviations from equilibrium? (*)

NB: discuss only deviations from ionization equilibrium; deviations from kinetic equilibrium (T_i-T_e; nonthermal electrons; cosmic rays, …) out of scope (*e.g.* collisionless shocks, feebleness of Coulomb interactions, …).

Ionizing plasmas: ionization balance too low for prevailing electron temperature (or photoionization parameter ξ)

Rough criterion:

low densities means: low collision frequency: ionization balance lags. Typically reach ionization equilibrium for **$n_e\ t > 10^{12}\ cm^{-3}\ sec$** (depends on ion)

Examples: young supernova remnants; stellar flares; IGM, …

(*) simplest diagnostic: if continuum gives T_e, compare to ionization balance….; trivial.

Average baryon density at z = 0: $n = 2 \times 10^{-7}$ cm^{-3}

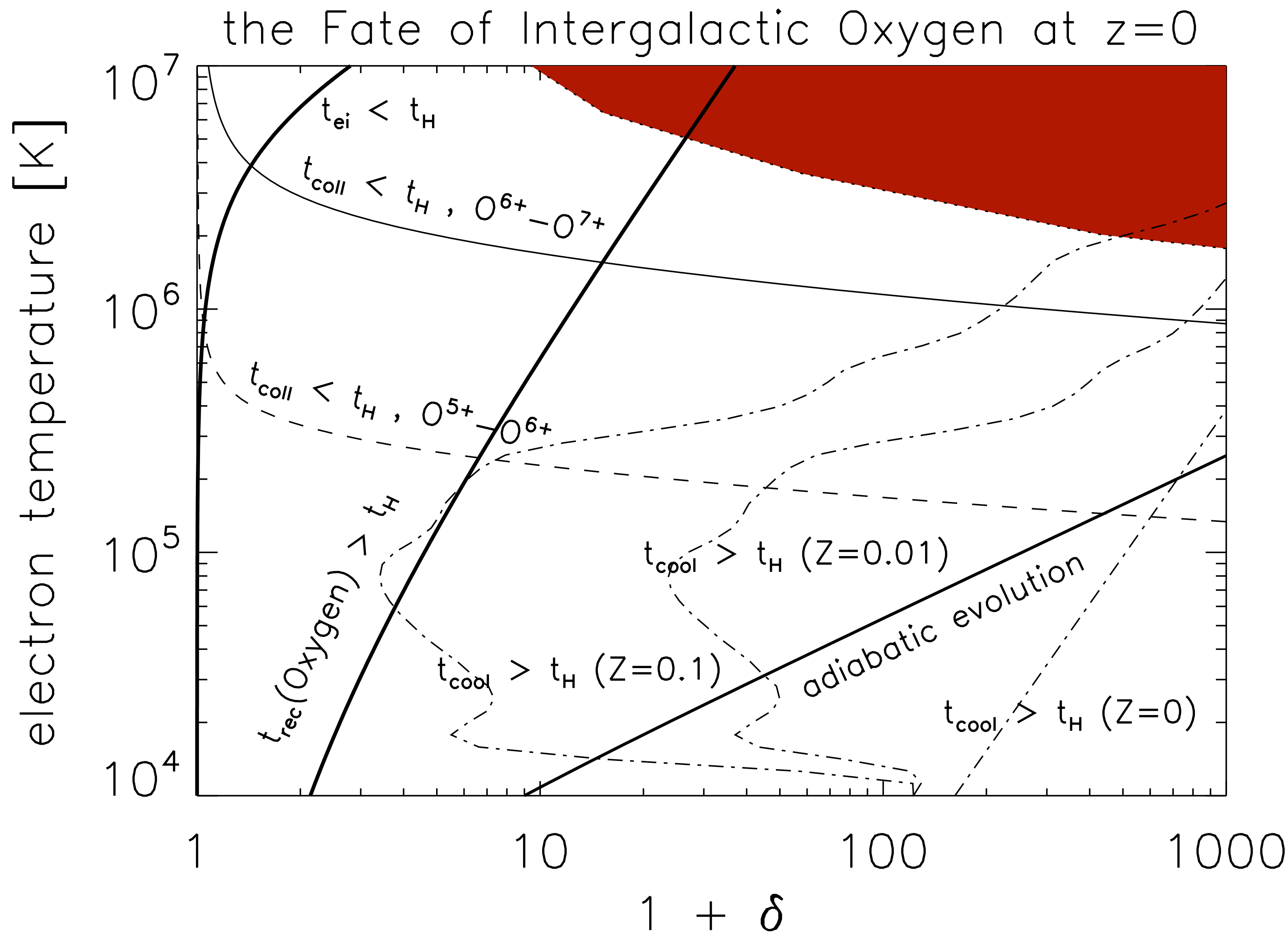

In the IGM, n_e is so low that equilibrium timescales may be longer than the age of the Universe!

Innershell excitations in (relatively) low charge ions

Example: excitation of n=1-2 in Be-, Li-, and He-like Fe (EBIT experiment)

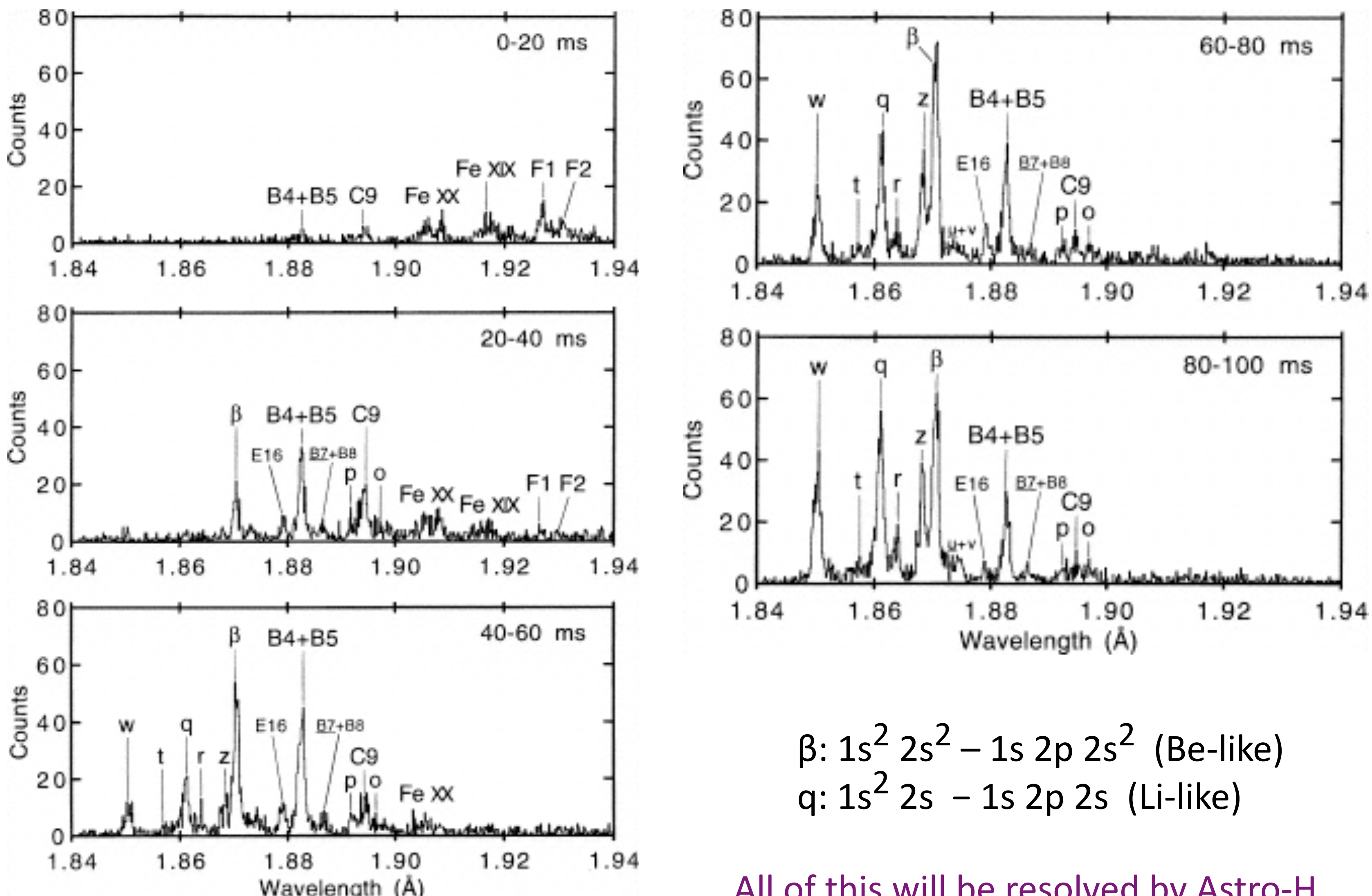

Decaux *et al.*, *ApJ*, **482**, 1076 (1997)

β: $1s^2\ 2s^2 - 1s\ 2p\ 2s^2$ (Be-like)

q: $1s^2\ 2s - 1s\ 2p\ 2s$ (Li-like)

All of this will be resolved by Astro-H

Also: He-like triplet shows only w, no x,y,z! no recombinations (yet)

Recombining plasmas: ionization balance too high for prevailing electron temperature (or photoionization parameter ξ)

Looks like a photoionized plasma:

He-like triplets will show bright x,y,z, compared to w;
May see RRC's, if the plasma is cool enough.

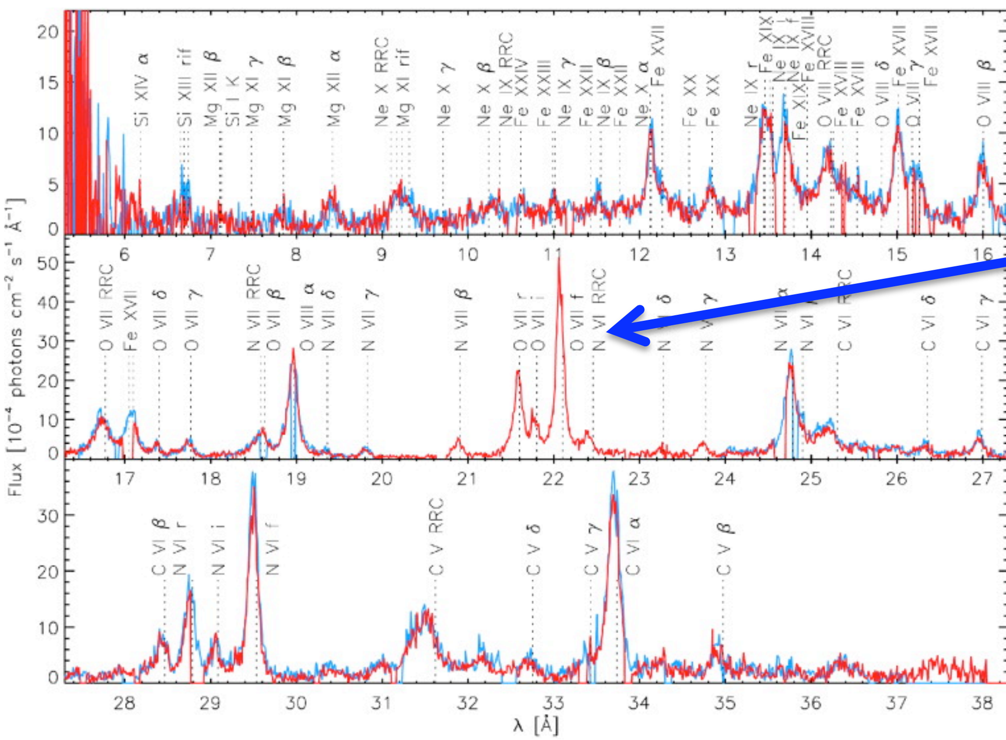

bright z; faint w

XMM-RGS NGC 1068 again

Recombining plasma in SNR IC 443 with Suzaku (?!)

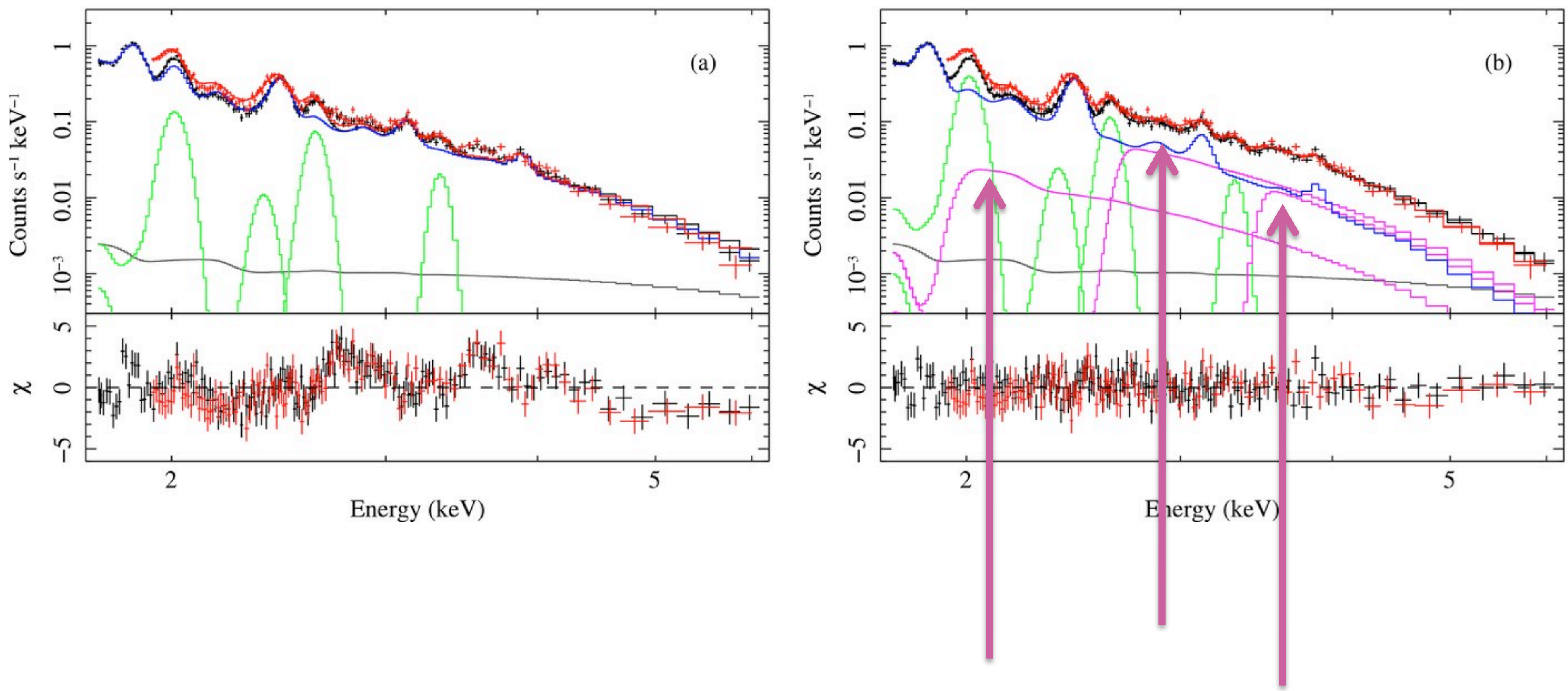

Yamaguchi *et al.*, *ApJL*, **705**, L6 (2009)

Radiative Transfer Issues

Plasmas of interest may be optically think in strong resonance lines
Two effects may be observable:

(1) scattering of resonance line photons
(2) scattering of continuum photons by strong resonance transitions

Lines with the highest (oscillator strength) x (astrophysical abundance):

He-like *w* in O and Fe; Fe XVII 2p-3d 15.014 Å (826 eV)

Maybe in clusters; elliptical galaxies; Type II AGN with outflow

(1) Resonance scattering in spherically symmetric diffuse source:
photons scattered out of line of sight compensated by photons scattered into line of sight further out (gas density low: no collisional destruction of photons, so total photon luminosity must be conserved):

image in resonance line photons will appear wider than image in optically thin radiation; but need angular resolution to see this! Not just spectral resolution!

(2) Scattering of continuum photons on strong resonance transitions in anisotropic situations (*e.g.* AGN outflow exposed to central continuum)

Will appear to enhance resonance lines; effect depends on velocity gradients!

Most extreme example: scattering of the X-ray background continuum by intergalactic OVII *w* – if you can resolve most of the point sources that make the background!

Finally: **Compton and Raman scattering of line photons** (in practice: Fe lines- scattering medium likely to be photoelectrically opaque at lower energies)
This will happen - we have seen it in X-ray binaries!
Analysis will reveal optical depth, electron temperature, angular distribution of scattering electrons/H-atoms, as seen from line source.

May give novel constraints on 'cold reflection' in AGN- important for relativistically distorted Fe emission lines (black hole spin, …)

Compton 'shoulder' on Fe Kα
(GX301-2, *Chandra* HETGS)

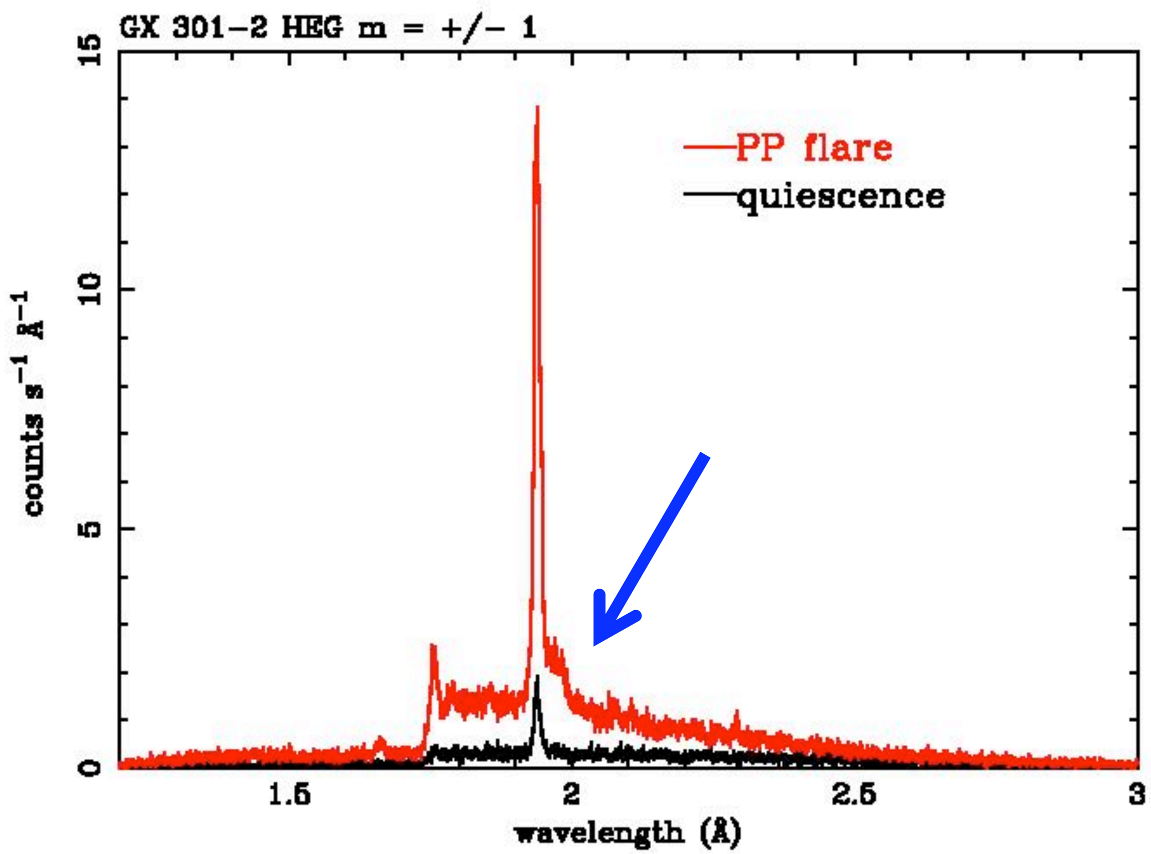

(Courtesy Masao Sako,then Stanford;
analysis: Watanabe *et al.*, *ApJL*, **597**, L37 (2003))

Width = 2 λ_C (electron)!! (NB: plot against wavelength if you suspect Compton scattering!!)

Compton's original experiment, in an astrophysical source…

Quiz: A Gallery of He-like Triplets

What conditions produce these triplet spectra?

1

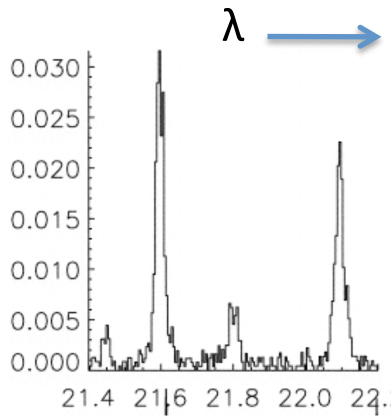

7

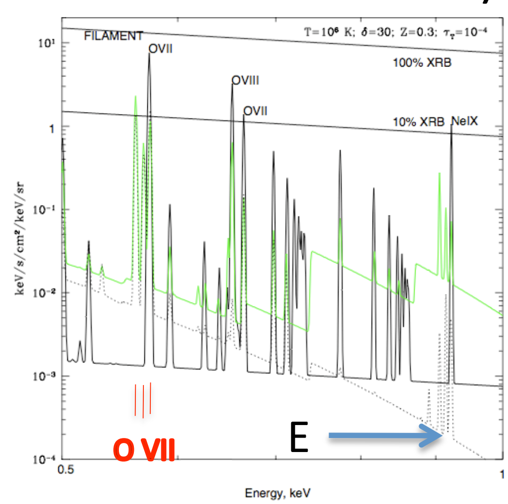

6

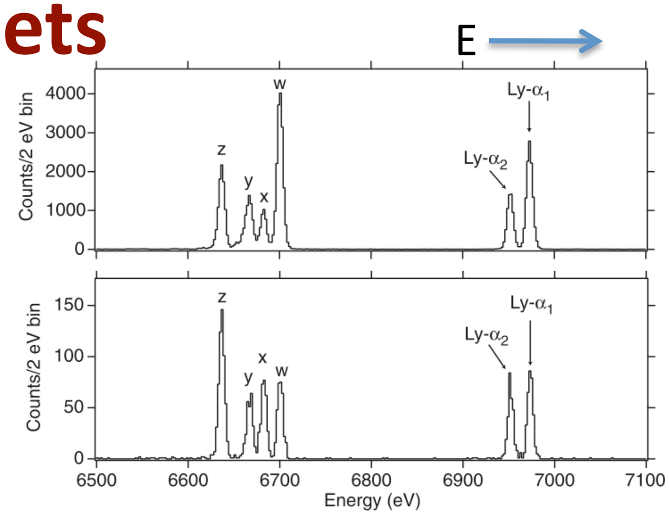

4

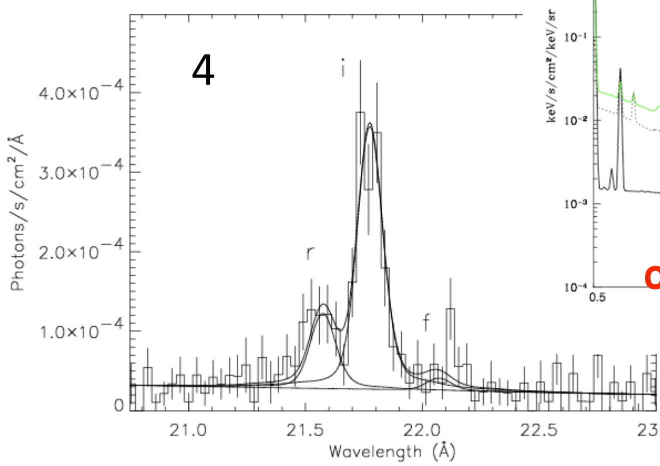

3

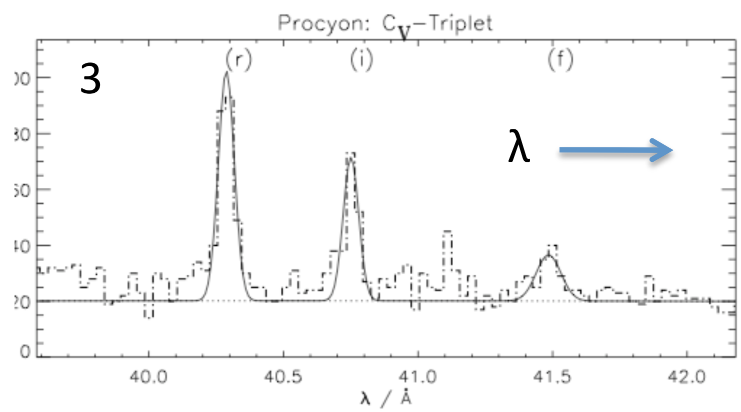

5

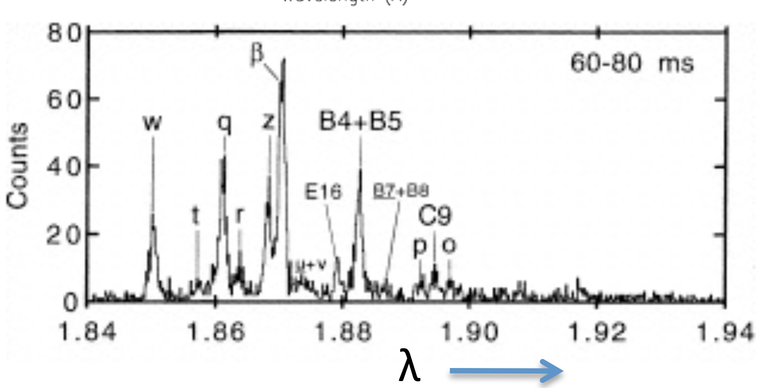

2

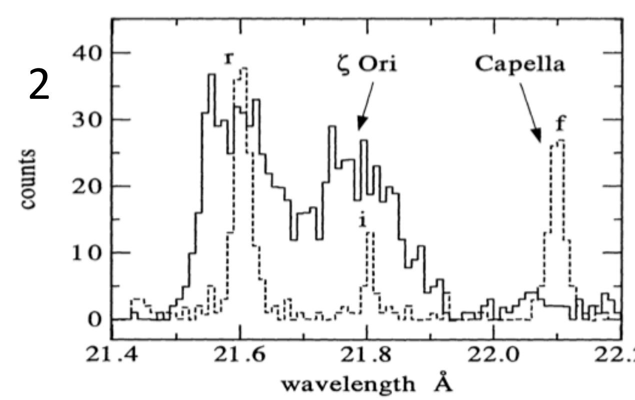

References to previous page:

1. Capella: Canizares *et al*., *ApJL*, **539**, L41 (2000)
2. ζ Ori: Waldron & Cassinelli, *ASP Conf. Proc*., **262**, 69 (2002)
3. Procyon: J.-U. Ness *et al*., A&A, **367**, 282 (2001)
4. EXO0748-676: Cottam *et al.*, *A&A*, **365**, L277 (2001)
5. EBIT: Decaux e*t al.*, *ApJ*, **482**, 1076 (1997)
6. EBIT: Wargelin *et al*., *Can. J.Phys*., **86**, 151 (2008)
7. IGM, theory: Churazov *et al.*, 2010arXiv1007.3263C